AIAA JOURNAL
Vol. 32, No. 11, November 1994

Growth of Multiple Cracks and Their Linkup in a Fuselage Lap Joint

Ripudaman Singh,* Jai H. Park,† and Satya N. Atluri‡
Georgia Institute of Technology, Atlanta, Georgia 30332

An issue of concern in aging aircraft is the growth of multiple cracks emanating from a row of fastener holes, typically in a pressurized aircraft fuselage lap splice. This multisite damage (MSD), or widespread fatigue damage, if allowed to progress, can suddenly become catastrophic. The understanding of the failure behavior dictates the level of compromise between safety and economy. The complexity of the structure due to various stiffening elements makes it unamenable to a simple direct analysis. A two-step elastic finite element fatigue analysis combining a conventional finite element method and the Schwartz-Neumann alternating method with analytical solutions is developed to understand fatigue growth of multiple cracks and to obtain a first estimate of the residual life of a stiffened fuselage shell structure with MSD in the riveted lap joint. The analysis procedure is validated by simulating a laboratory fatigue test on a lap joint in a flat coupon. Both the coupon and the shell panel are found to have fatigue lives only up to the first linkup of neighboring crack tips.

Introduction

THE phenomenon of growth of multiple cracks in a widespread fatigue damage scenario and their linkup to form dominant cracks in primary aircraft structural components have been a matter of concern among engineers trying to assess the structural integrity of aging fleets. The authors and their colleagues at Georgia Institute of Technology are developing state-of-the-art computational tools for residual strength/fatigue life estimations of damaged structures. These tools are expected to be extremely efficient from both manpower as well as computer resource requirement points of view. The subject of study in this paper is the fatigue growth and linkup of multiple cracks emanating from a row of fastener holes in a bonded/riveted longitudinal lap joint in a pressurized stiffened fuselage shell structure.

A multibay shell panel of a typical narrow body fuselage, with all of its structural features and a lap splice, is modeled. An arbitrary initial crack configuration, at the outer critical row of fasteners, is chosen as a starting point. The fatigue loading applied is the cyclic pressurization of the fuselage. The pressurization induces a hoop stress that is transferred across the shell skins mainly through the lap joint and partly through the circumferential stiffening elements, i.e., frames and tear straps. In a perfectly bonded lap, the adhesive transfers most of the load through shear, but with aging the bond may deteriorate and the load is transferred primarily through the countersunk rivets. The cracks grow up to a certain length under the fastener heads and make the detection difficult. When the cracks start showing up from under the head of the fastener, they are long enough, have a reasonably high growth rate, and can soon become catastrophic, through linkup.

The geometric complexity and the arbitrarily large number of cracks emanating at a row of fastener holes make a direct numerical analysis extremely expensive. The authors have earlier developed a global-local static analysis approach in which the load flow pattern through the damaged panel is first determined using a regular finite element method (FEM) and then the cracked portion of the skin is isolated. To this local model of the cracked skin, which is subjected to tractions as determined, the Schwartz-Neumann alternating FEM is applied to obtain the crack tip parameters.[1] This FEM analytical alternating technique is extended in this paper to fatigue analysis. The multiple cracks emanating from a row of fastener holes are simulated to grow under fatigue loading during the local analysis of the cracked rivet holes. The global analysis of the shell panel is repeated whenever the crack configuration changes are significant enough to alter the load flow pattern through the damaged splice; this could be due to crack growth or linkup of two cracks. Net section ligament yielding is considered to be the linkup criterion under the fatigue loading of these closely spaced cracks. Before investigating the problem of multiple crack growth in a fuselage panel, we validated the developed technique and the code by simulating a laboratory fatigue test to investigate the fatigue linkup of multisite damage (MSD) in a typical lap joint coupon.[2]

Problem Definition

Shell Panel

Consider a typical narrow body fuselage shell stiffened longitudinally by stringers and circumferentially by frames and tear straps. Tear straps are present at all frame locations and midframe

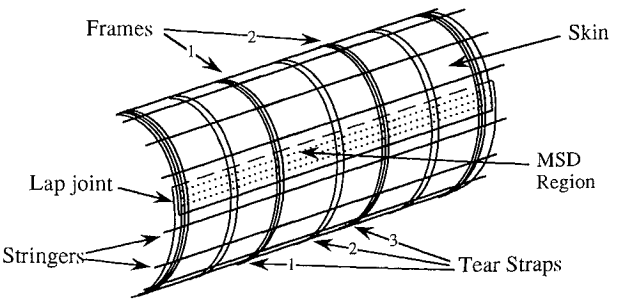

Shell Panel for Global Analysis

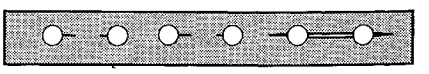

Cracked Skin Segment for Local analysis

Fig. 1 Shell panel configuration.

Received Dec. 13, 1993; revision received May 20, 1994; accepted for publication May 20, 1994.

*Postdoctoral Fellow, FAA Center of Excellence for Computational Modeling of Aircraft Structures.

†Visiting Professor, FAA Center of Excellence for Computational Modeling of Aircraft Structures; currently Professor, Department of Industrial Safety Engineering, Chungbuk National University, Cheongju 360-763, Republic of Korea.

‡Institute Professor and Regents' Professor of Engineering, FAA Center of Excellence for Computational Modeling of Aircraft Structures. Fellow AIAA.

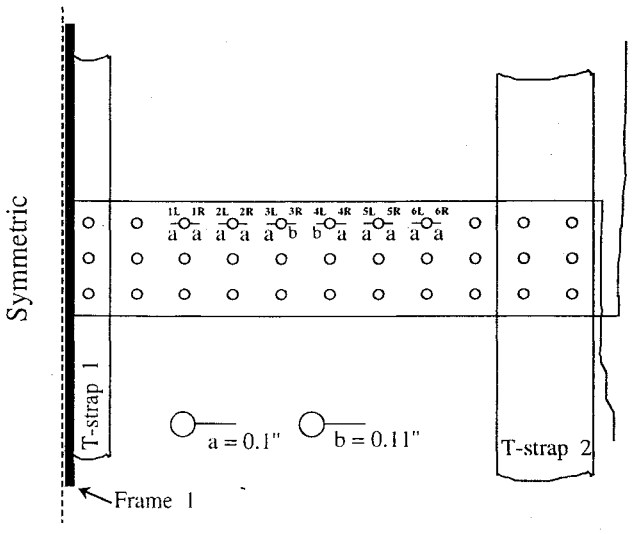

Fig. 2 Initial crack configuration in the shell panel.

stations. Refer to Fig. 1 for a typical configuration. The geometrical details are as follows:

Shell radius R	74.0 in. (187.96 cm)
Shell skin thickness t	0.036 in. (0.0915 cm)
Distance between frames	20.0 in. (50.8 cm)
Distance between stringers	9.25 in. (23.495 cm)
Distance between tear straps	10.0 in. (25.4 cm)
Width of tear straps	2.0 in. (5.08 cm)
Thickness of tear straps t_t	0.036 in. (0.0915 cm)
Frame area	0.160 in.^{2} (1.032 cm^2)
Frame moment of inertia	0.120 in.^{4} (5.0 cm^4)
Frame neutral axis offset	3.15 in. (8.0 cm)
Stringer area	0.186 in.^{2} (1.2 cm^2)
Stringer moment of inertia	0.040 in.^{4} (1.67 cm^4)
Stringer neutral axis offset	0.78 in. (1.98 cm)
Fuselage internal pressure	9.0 psi (62 kPa)
Rivet diameter D	0.15625 in. (0.397 cm)
Pitch of rivets	1.0 in. (2.54 cm)
Material	Al 2024-T3

Consider a longitudinal lap joint with the following particulars:

Length of overlap	3.0 in. (7.62 cm)
Number of rivet rows	3
Pitch of rivets	1.0 in. (2.54 cm)
Number of rivets in each bay	20 × 3
Rivet diameter D	0.15625 in. (0.397 cm)
Adhesive layer thickness t_a	0.0025 in. (0.00635 cm)
Material	Al 2024-T3

The material properties of Al 2024-T3 are taken as follows:

Young's modulus E	10.5×10^3 ksi (72.3 GPa)
Shear modulus G	4.2×10^3 ksi (28.9 GPa)
Poisson's ratio ν	0.32
Yield strength σ_y	47.0 ksi (323 MPa)
Ultimate tensile strength σ_u	64.0 ksi (440 MPa)
Crack tip linkup stress $(1/2)(\sigma_y + \sigma_u)$	55.5 ksi (381 MPa)
Elongation	18%
Fracture toughness K_{IC}	93.0 ksi $\sqrt{\text{in.}}$ (102 MPa $\sqrt{\text{m}}$)

The adhesive shear modulus is G_a = 109 ksi (751 MPa).

Consider a panel of this shell, consisting of five frames (nine tear straps), seven stringers, and a longitudinal lap joint. Initially all of the stiffening elements are presumed to be intact. As the cracks grow and link up to form a dominant crack, these stiffeners get overloaded and may fail. The adhesive is treated to be degraded to 1% of its original strength due to aging, so that the fasteners transfer all of the load through the joint. Consider the problem of multiple cracks of finite lengths emanating from the outer critical row of fastener holes in two adjacent bays, across a frame (called frame 1). Figure 2 shows the initial crack configuration of six cracks (with two tips each) numbered 1L to 6R (L for left and R for right) emanating from six fastener holes. All of the MSD cracks in a bay are considered in the same half of the bay, i.e., between two tear straps, numbered T-strap 1 and 2 in this case. The crack lengths of 0.10 in. (0.254 cm) are chosen to typically represent a situation where the cracks are hidden well under the countersunk head of the fastener. The cracks' lengths are measured from the center of the hole and thus include the fastener radius. At the central ligament, the cracks 3R and 4L have been specifically chosen to be a length of 0.11 in. (0.279 cm) so as to insure the first linkup at this location. The configuration is chosen to be symmetric about the frame for ease of analysis. Thus we need to analyze only one-half of the damaged panel, i.e., three frames and five straps. The fatigue loading applied is the cyclic pressurization of the shell from 0.0 to 9.0 psi (62 KPa). Under this loading, the MSD cracks are expected to link up to form two long cracks, one in each bay, which will further link up at the frame location to form a single dominant two-bay crack. Fatigue growth of the initial set of cracks is considered up to the formation of a full two-bay-long crack.

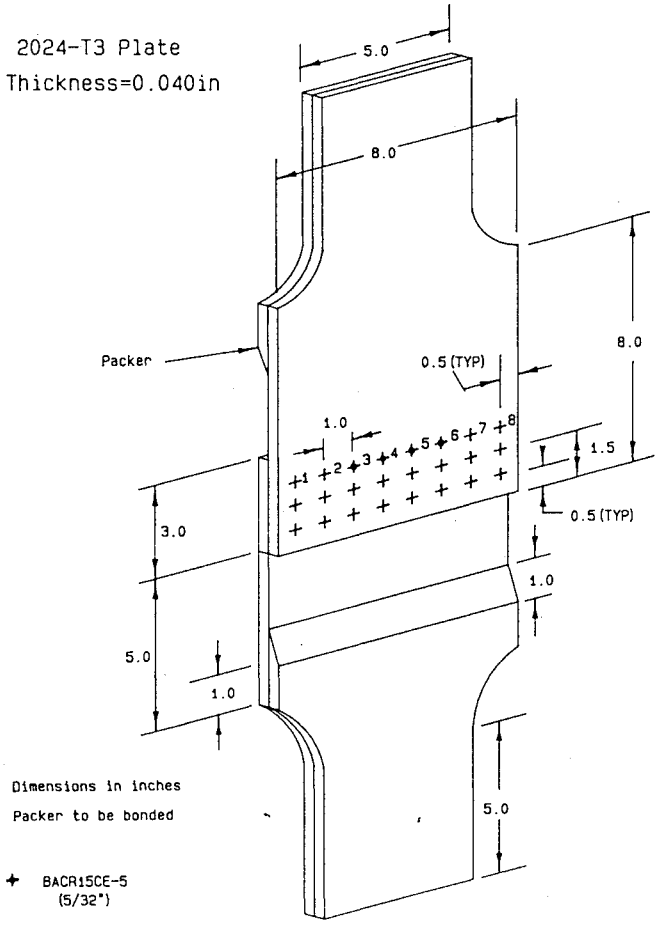

Fig. 3 Flat coupon lap joint configuration.

Whenever there is a crack linkup, and if there is no crack emanating at the other end of the hole, it can be treated as having arrested, and fatigue growth has no meaning beyond this point. However, in reality there could be small cracks and they will grow, and so to perform fatigue analysis, very small cracks are presumed to exist at all other fastener holes but are considered in the analysis only when the dominant crack tip comes close enough.

Coupon Configuration

Laboratory test of MSD fatigue crack growth at a lap joint in a flat coupon,[2] performed at the Aeronautical Research Laboratory, Melbourne, Australia, has been simulated to verify the analysis procedure. The configuration for the coupon is shown in Fig. 3 (taken from the original munscript[2]). The sheet thickness is 0.04 in. (0.1 cm) in the present case. The width of 8 in. (20.32 cm) represents the portion of the skin between the tear straps. The lap

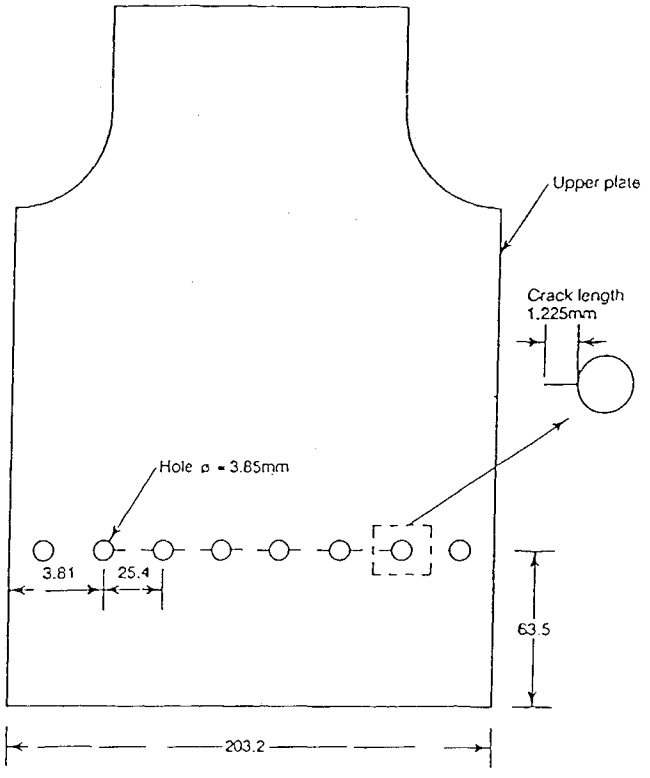

Fig. 4 Initial crack configuration in the coupon.

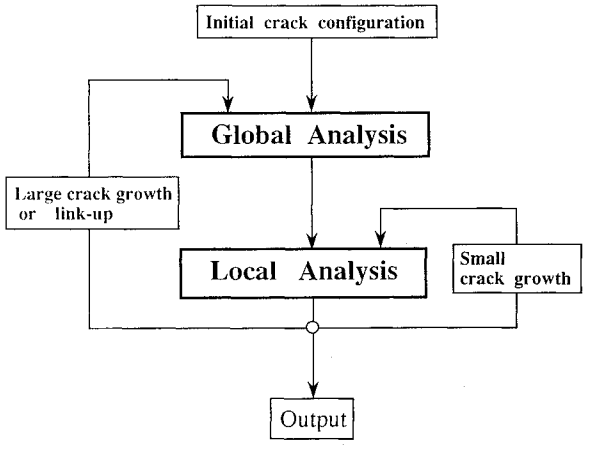

Fig. 5 Schematic of the global-local fatigue analysis.

splice configuration is identical to that in the shell panel joint, with a fastener diameter of 5/32 in. (0.3968 cm). The initial crack configuration considered is shown in Fig. 4. In the experiments the cracks were generated using an electrical spark erosion technique. The cracks were taken to be 0.047244 in. (0.12 cm) long so that the defect was obscured by the fastener head and represents a possible undetectable flaw. This would correspond to a crack tip distance of 0.124 in. (0.315 cm) from the hole center. In the experiment the local bending was minimized by testing the specimens bonded back to back and separated by a honeycomb core 0.492 in. (1.25 cm) thick. The fatigue loading on the sheet is uniaxial tension varying between 0.67 and 13.4 ksi (4.61–92 MPa), corresponding to a stress ratio of 0.95. The sheet material is Al 2024-T3.

Analytical Approach

The analytical approach employed for the present study consists of a repetitive global-local analysis. A global finite element analysis is first carried out on the initial crack configuration to determine the fastener loads and the sheet stresses some distance away in the meridional direction from the longitudinal crack axis. A local analysis on the isolated, loaded, and cracked skin segment is then carried out to obtain the crack tip parameters using the Schwartz-Neumann finite element alternating method (FEAM). With the evaluated crack tip parameters, the crack is allowed to grow as per the Paris equation. The local analysis is performed for crack increments small enough not to alter the load flow through the panel. Whenever the crack growth is significant to effect the load flow pattern or the crack linkup occurs, a fresh global analysis is performed to update the fastener loads and the sheet stresses. The global analysis procedure is same as presented earlier,[1] but is repeated here for the sake of completeness. The alternating method for local analysis has been further improved and the details are presented here. Schematically the procedure is shown in Fig. 5.

Global Analysis

Conventional linear elastic finite element analysis of the multibay stiffened shell panel with cracks is performed as a part of the global analysis. The FEM model is briefly described next:

The fuselage skin is modeled by four-noded shell elements with five degrees of freedom (DOF) per node. The element used is strain based and was developed by Ashwell and Sabir.[3] Tear straps are also modeled using the same element. The frames and stringers are modeled as two-noded, three-DOF-per-node, curved/straight beam elements with their shape functions being degenerated from those of shell elements. This is done to insure compatibility within the stiffeners and the sheet. The cracks are incorporated into the problem at this level, as unconnected nodes belonging to respective elements. For the purpose of the present global analysis, the crack tip singularity is not modeled since we are not interested in the SIF at this stage. Appropriate account of the crack tip singularities is taken during the local analysis. The fasteners are modeled as two-DOF connections between the corresponding nodes in the upper and the lower skins, and the stiffness is represented by the empirical relation developed by Swift[4]:

$$K_F = \frac{ED}{[A + C\,(D/t_1 + D/t_2)\,]} \tag{1}$$

with $A = 5.0$ and $C = 0.8$ for Al rivets. Wherever there is a crack that bridges across fastener holes, the stiffness of the fastener in the direction of the crack axis is set to zero as the fastener will not be able to carry a load in that direction. The adhesive is also modeled as a two-noded, two-DOF-per-node connection between the sheets. The adhesive stiffness is modeled as

$$K_a = \mu_d \frac{\text{area}}{t_a/G_a + (3/8)\,(t_1/G + t_2/G)} \tag{2}$$

where μ_d is the degradation factor. The values of 0 and 1 represent total degradation and no degradation, respectively. A value of 0.1 means 90% degradation. "Area" represents the bond area being lumped at the nodal connections. Appropriate multipoint constraints have been imposed to prevent crisscrossing of sheet nodes in the lap joint zone. The fuselage internal pressure is applied as a uniformly distributed normal outward load on the shell panel. The four edges of the panel are permitted to undergo only radial displacement in the cylindrical system. A typical problem size for the configurations considered is on the order of 15,000 DOF, and the computer time is on the order of minutes on an HP 9000/700 series workstation.

Local Analysis

From the global analysis, the skin segment containing the cracks, holes, and fasteners of interest is isolated with corresponding sheet stresses. The fastener holes are now modeled as circular, and the bearing loads are distributed as sinusoidal variation over one-half of the circumference of the hole, with the peak of the sinusoid being in the direction of the fastener load as determined from the global analysis. The stresses due to the misfit of the rivet, as well as the initial stresses in the sheet due to the riveting process

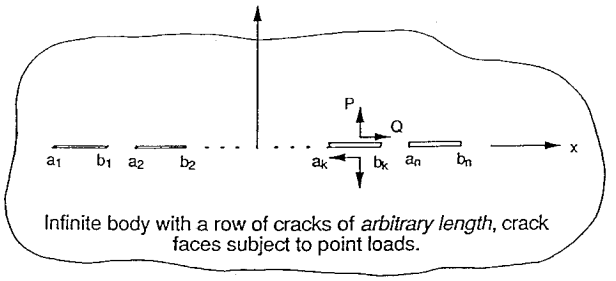

a) The analytical solution for the above problem has been generated.

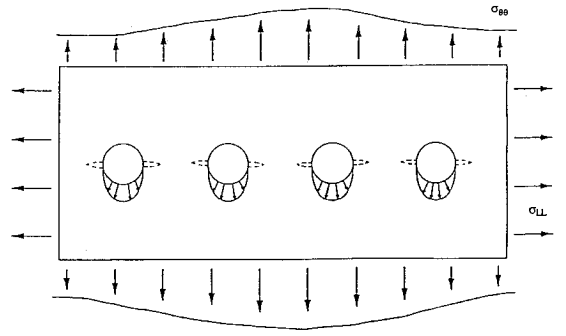

b) Finite element solution for a finite plate with a row of circular holes (*No Cracks*).

Fig. 6 Finite element alternating methodology.

itself, can also be accounted for at this stage. This problem is solved using the Schwartz-Neumann FEAM, presented in detail in an earlier paper by Park and Atluri,[5] which involves two solutions.

1) An analytical solution to the problem of a row of cracks of arbitrary lengths in an infinite sheet, with crack faces being subjected to arbitrary tractions: This basic solution has been recently redeveloped to improve the accuracy of the stress field near the crack surface. The details of this new solution are given in the next subsection.

2) A finite element solution for a strip with/without a row of holes, but without cracks, subjected to sheet stresses: Eight-noded isoparametric elements with two DOF per node are employed in this finite element analysis.

The analytical-numerical alternating technique is illustrated in Fig. 6 and is briefly described as next:

1) Solve the strip problem under edge tractions and pin bearing loads, without modeling cracks, using convention FEM with eight-noded isoparametric elements.

2) To create the traction-free crack surfaces, erase the stresses as found in step 1, on the crack surfaces, using the analytical solution for an infinite sheet containing multiple collinear cracks (discussed in the next section). Determine the SIF at all of the crack tips in the domain.

3) Corresponding to the solution in step 2, determine the residual tractions at the surfaces of all of the holes and the outer boundaries of the finite strip.

4) Using the FEM, obtain the stresses at the crack locations, corresponding to the reversed tractions obtained in step 3.

5) Repeat steps 2–4 until increments in SIF resulting from step 4 are vanishingly small. By summing up all of the contributions, total SIF for each crack tip can be obtained.

The crack tip stress intensity factors and the stress field are obtained from this local analysis. The net ligament stress for any ligament is obtained by taking an average over the ligament length. To compute the plastic zone size, the Irwin's formula does not seem to give a reasonable approximation, probably due to the complexity of geometry and vicinity of other cracks/loaded holes. Consequently, the plastic zone size is estimated from the computed stress field (which has the elastic singular variation near the crack tip) by doubling the distance from crack tip to the point where the stress falls to yield stress to account for the redistribution of the elastic stress field due to plasticity. This is only an approximation in lieu of performing a full elastic-plastic analysis. Such full elastic-plastic analysis of an MSD cracking situation has been completed recently at Georgia Tech. This most recent analysis, to be published shortly elsewhere, gives the most accurate representation of plastic zone sizes.

The critical pressure for the fuselage is that value of applied pressure differential for which either the crack tip becomes unstable or the ligament between two crack tips fails. For linear elastic analysis this can be computed directly from the obtained values of K_1 and average ligament stress σ_{av}:

$$\text{critical pressure differential} = \text{applied pressure} \times K_{1C}/K_1$$

$$\text{critical pressure differential} = \text{applied pressure} \times \frac{\text{linkup stress}}{\sigma_{av}}$$

The linkup stress is taken to be the average of yield and ultimate strength.[8]

Basic Analytical Solution

In the local analysis, it is important to obtain accurate (singular, elastic) stress fields near the crack tips. A solution has been developed to obtain this for the case of multiple collinear cracks with arbitrary surface tractions. The arbitrary tractions can be approximately treated as superposition of various piecewise constant tractions; one such is shown in Fig. 7.

Consider the problem where n cracks are located along the x axis, and a uniform normal stress p_o and shear stress q_o are applied in the region $d_1 \le x \le d_2$ on the kth crack surface as shown in the figure. The solution can be obtained by using the method given by Muskhelishvili.[9] The complex stress functions are given by :

$$\Phi(z) = \frac{(-p_o + iq_o)}{2\pi i X(z)}\left[\int_{d_1}^{d_2} \frac{X^+(t)}{t-z}\,dt + i(c_1 z^{n-1} + c_2 z^{n-2} + \ldots + c_n)\right] \tag{3}$$

$$\Omega(z) = \Phi(z)$$

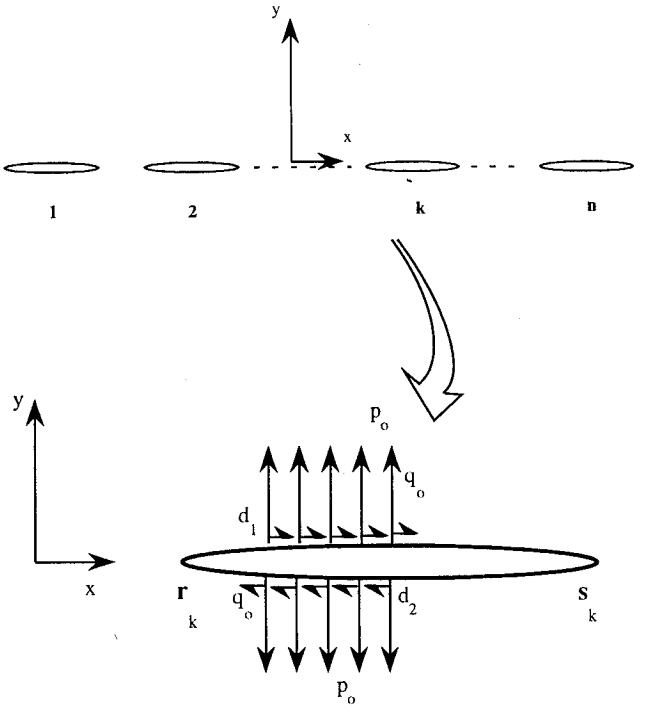

Fig. 7 Multiple collinear cracks with constant surface tractions over a small zone in *k*th crack.

where

$$X(z) = \prod_{i=1}^{n} \sqrt{z-r_i}\,\sqrt{z-s_i} \tag{4}$$

and the branch is chosen as $X(z)$ and becomes z^n for large $|z|$. The upper index + refers to the boundary values on the upper surface of the crack. The stresses can be obtained by the following relations:

$$\sigma_x + \sigma_y = 2\,[\Phi(z) + \overline{\Phi(z)}]$$
$$\sigma_y - i\sigma_{xy} = \Phi(z) + \Omega(\bar{z}) + (z-\bar{z})\,\overline{\Phi'(z)} \tag{5}$$

Since the integral in Eq. (3) cannot be readily expressed in a closed form for an arbitrary number of cracks, we make the following assumption to simplify the problem: the length (d_2-d_1) is so small that within $d_1 \le t \le d_2$ the $X^+(t)$ can be expressed approximately as

$$X^+(t) \simeq X^+(d)\frac{\sqrt{t-t_k}}{\sqrt{d-t_k}} \tag{6}$$

where $d = (d_1 + d_2)/2$, and t_k is the x coordinate of the nearest crack tip from d. Consequently, the t_k can be r_k or s_k in this problem. By substituting Eq. (6) into Eq. (3), we obtain

$$\Phi(z) = \frac{(-p_o + iq_o)}{2\pi i X(z)}\{X^+(d)\,[I(z,d_2) - I(z,d_1)] + i(c_1 z^{n-1} + c_2 z^{n-2} + \ldots + c_n)\}$$
$$\Omega(z) = \Phi(z) \tag{7}$$

where

$$I(z,t_0) = 2\frac{\sqrt{t_0-t_k}}{\sqrt{d-t_k}} + \frac{\sqrt{z-t_k}}{\sqrt{d-t_k}}\,\ln\frac{\sqrt{t_0-t_k}-\sqrt{z-t_k}}{\sqrt{t_0-t_k}+\sqrt{z-t_k}} \tag{8}$$

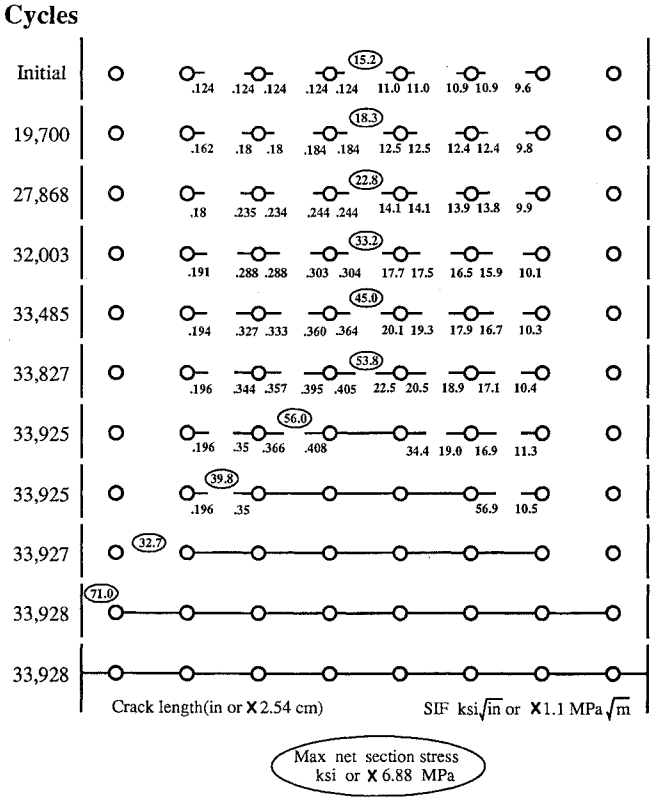

Fig. 8 Comprehensive picture of MSD crack growth in the coupon.

Table 1 Rivetwise load (in pounds or × 4.45 N) distribution in the outer row at various stages of the panel fatigue failure

	Rivet no.							
Cycles	1	2	3	4	5	6	7	8
Initial	172	172	172	172				
19,700	182	184	147	152				
27,868	182	185	140	144				
32,003	183	186	135	139				
33,485	185	188	129	133		Symmetric		
33,827	187	191	126	128				
33,925	188	193	125	124				
			First linkup					
33,925	196	205	133	98				
33,927	235	262	113	43				
33,928	290	352	51	29				
33,928	612	78	36	21				

Table 2 Row-wise load (in pounds or × 4.45 N) distribution at various stages of the panel fatigue failure

Cycles	Row 1	Row 2	Row 3
Initial	1370	1118	1370
19,700	1328	1157	1372
27,868	1306	1167	1384
32,003	1286	1177	1395
33,485	1272	1184	1401
33,827	1265	1188	1405
33,925	1261	1190	1407
	First linkup		
33,925	1268	1184	1405
33,927	1314	1155	1388
33,928	1447	1065	1330
33,928	1494	1020	1296

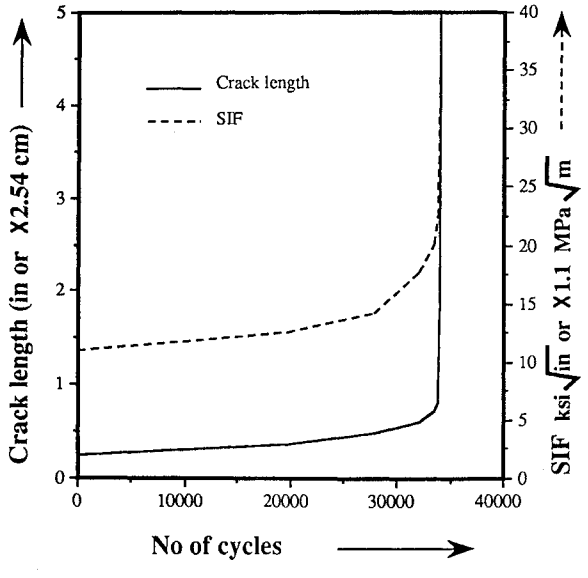

Fig. 9 SIF and crack length variation with number of cycles.

All of the square-root functions are interpreted as complex variable functions.

The coefficients $c_1, c_2, \ldots, c_n$ in Eq. (7) can be determined from the single-valuedness condition on the displacement field, which is expressed as follows:

$$c_1\int_{r_j}^{s_j}\frac{t^{n-1}}{X(t)}\,dt + c_2\int_{r_j}^{s_j}\frac{t^{n-2}}{X(t)}\,dt + \cdots + c_n\int_{r_j}^{s_j}\frac{1}{X(t)}\,dt$$
$$= i\int_{r_j}^{s_j}\frac{X(d)}{X(t)}\,[I(t,d_2) - I(t,d_1)]\,dt, \qquad j = 1, 2, \ldots, n \tag{9}$$

The SIF at the tips of multiple cracks can now be obtained. For the crack tips at $x = r_k$ and at $x = s_k$ they are, respectively,

$$K_I - iK_{II} = \lim_{x \to r_k} \sqrt{2\pi (r_k - x)}\ (\sigma_y - \sigma_{xy})$$

$$= (p_o - iq_o) \sqrt{\frac{2}{\pi}} \frac{1}{X_2} \left[\frac{X_1}{\sqrt{c - r_k}} + iP_n(r_k) \right]$$

$$K_I - iK_{II} = \lim_{x \to s_k} \sqrt{2\pi (r_s - x)}\ (\sigma_y - \sigma_{xy})$$

$$= (p_o - iq_o) \sqrt{\frac{2}{\pi}} \frac{1}{X_4} \left[\frac{X_3}{\sqrt{s_k - c}} + iP_n(s_k) \right]$$

where

$$X_1 = \prod_{m=1,\ m \neq k}^{n} \sqrt{c - r_m} \prod_{m=1}^{n} \sqrt{c - s_m}$$

$$X_2 = \prod_{m=1,\ m \neq k}^{n} \sqrt{r_k - r_m} \prod_{m=1}^{n} \sqrt{r_k - s_m}$$

$$X_3 = \prod_{m=1}^{n} \sqrt{c - r_m} \prod_{m=1,\ m \neq k}^{n} \sqrt{c - s_m}$$

$$X_4 = \prod_{m=1}^{n} \sqrt{s_k - r_m} \prod_{m=1,\ m \neq k}^{n} \sqrt{s_k - s_m}$$

$$P_n(z) = \sum_{j=0}^{n} c_j z^{n-j}$$

By using the solutions of this problem as Green functions, we can obtain the stress fields and SIF's collinear multiple cracks, each of arbitrary length, and each being subjected to arbitrary tractions.

Crack Growth

The crack growth rate considered is represented by the equation

$$\frac{da}{dN} = [A]\{\Delta K\}^n \tag{10}$$

The values of A and n are obtained from the experimental data.[10] These are

$$A = 3.64 \times 10^{-12}$$
$$n = 6.0 \tag{11}$$

where ΔK is in ksi $\sqrt{\text{in.}}$ and a is in inches.

Results and Observations

Coupon Problem

The fatigue growth analysis of MSD in a lap joint in a flat coupon of Fig. 3 with an initial crack configuration of Fig. 4 is carried out as per the procedure discussed in the preceding sections. The local and the global analyses are performed at crack length increments of 0.015 in. (0.0381 cm) and 0.060 in. (0.1524 cm), respectively. The comprehensive picture of the fatigue damage is shown in Fig. 8. Each stage marked by the number of fatigue cycles represents a state when the fresh global analysis was carried out to update the load distribution. Since the problem is symmetric, only

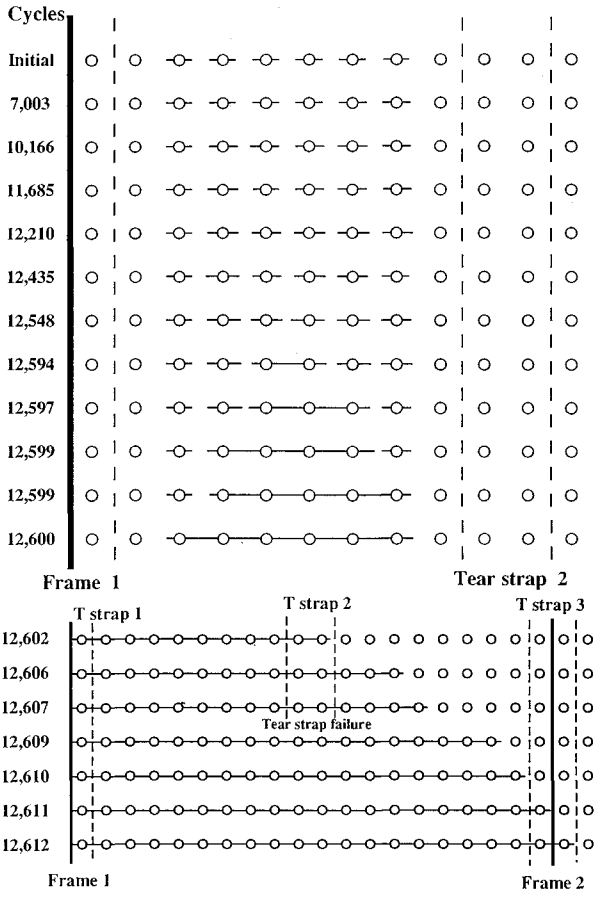

Fig. 10 Pictorial representation of fatigue damage in the shell panel.

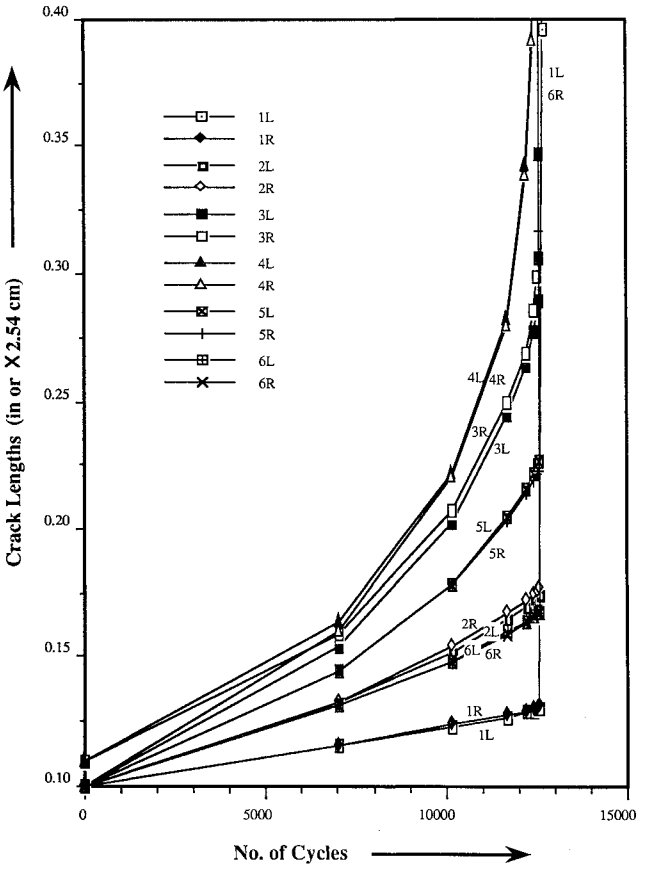

Fig. 11 Fatigue crack growth of the 12 cracks in the shell panel.

Table 3 Crack lengths and the crack tip SIF at various stages of fatigue

	MSD crack lengths,[a] in. or × 2.54 cm											
Cycles	1 L	1 R	2 L	2 R	3 L	3 R	4 L	4 R	5 L	5 R	6 L	6 R
Initial	0.100	0.100	0.100	0.100	0.100	0.110	.0110	0.100	0.100	0.100	0.100	0.100
7,003	0.116	0.116	0.132	0.133	0.154	0.159	0.164	0.160	0.145	0.144	0.131	0.131
10,166	0.123	0.124	0.152	0.154	0.203	0.207	0.222	0.220	0.178	0.178	0.148	0.148
11,685	0.127	0.128	0.165	0.167	0.245	0.249	0.282	0.280	0.205	0.204	0.160	0.159
12,210	0.129	0.129	0.170	0.172	0.264	0.269	0.342	0.338	0.216	0.214	0.164	0.164
12,435	0.129	0.130	0.173	0.175	0.277	0.286	0.403	0.392	0.222	0.219	0.166	0.166
12,548	0.130	0.130	0.174	0.176	0.285	0.299	0.465	0.442	0.225	0.222	0.168	0.168
12,594	0.130	0.131	0.175	0.177	0.289			0.475	0.226	0.223	0.168	0.168
12,595	0.130	0.131	0.175	0.177	0.306			0.491	0.227	0.223	0.168	0.168
12,597	0.130	0.131	0.175	0.177	0.347					0.223	0.168	0.168
12,598	0.130	0.131	0.175	0.177	0.457					0.317	0.168	0.168
12,599	0.130	0.131	0.175							0.479	0.168	0.168
12,599	0.130	0.131	0.175				Linkup					0.168
12,600	0.130											0.168
	MSD crack tip SIF (ksi-$\sqrt{\text{in.}}$ or × 1.1 MPa-$\sqrt{\text{m}}$											
Cycles	1 L	1 R	2 L	2 R	3 L	3 R	4 L	4 R	5 L	5 R	6 L	6 R
Initial	9.3	9.4	10.6	10.6	11.8	11.8	12.0	12.1	11.4	11.3	10.5	10.5
7,003	9.3	9.4	11.2	11.3	13.4	13.4	14.0	14.0	12.5	12.5	11.0	11.0
10,166	9.4	9.5	11.7	11.7	14.6	14.6	15.9	15.9	13.2	13.2	11.5	11.5
11,685	9.5	9.5	11.9	12.0	14.9	15.3	19.1	19.0	13.6	13.4	11.6	11.6
12,210	9.5	9.6	12.1	12.2	16.1	16.9	22.0	21.6	13.8	13.4	11.8	11.8
12,435	9.6	9.7	12.2	12.3	16.5	18.4	24.9	23.8	14.2	13.4	11.9	11.9
12,548	9.6	9.7	12.3	12.4	17.0	20.1	28.3	26.2	14.6	13.3	12.0	11.9
12,594	10.1	10.3	11.9	11.5	40.8			40.6	14.5	12.9	12.7	12.6
12,595	10.2	10.3	11.6	11.1	43.1			42.7	15.1	12.7	12.8	12.6
12,597	10.8	10.9	11.7	11.0	55.8					54.5	11.4	12.4
12,598	11.0	11.2	10.8	11.2	59.6					59.5	10.6	11.6
12,599	11.2	10.2	71.4							73.5	10.8	10.4
12,599	11.6	10.6	80.4				Linkup					79.1
12,600	78.8											64.6

[a]L= left, R = right.

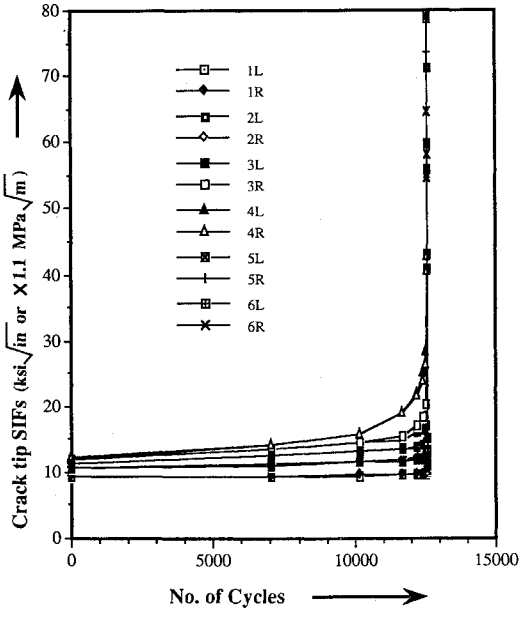

Fig. 12 Crack tip SIFs of the 12 cracks in the shell panel.

Table 4 Frame and tear strap loads at various stages of fatigue

	Frame and tear strap loads, lb or × 4.45 N				
Cycles	Frame 1	Tear strap 1	Tear strap 2	Tear strap 3	Frame 2
Initial	1019	31	264	30	1010
7,003	1019	31	264	30	1010
10,166	1020	31	265	30	1010
11,685	1021	32	265	30	1010
12,210	1021	32	266	30	1010
12,435	1021	32	266	30	1010
12,548	1022	32	267	30	1010
12,594	1028	34	269	29	1010
12,595	1029	34	269	29	1010
12,597	1037	36	278	29	1011
12,598	1040	37	282	28	1011
12,599	1067	46	291	27	1011
12,599	1082	50	327	26	1011
12,600	1110	57	357	25	1012
12,606	2106	612	3178	–54	1080
12,607	2110	613	3474	–60	1083
12,609	3185	1031	Fail	166	1636
12,610	3314	1071		428	2038
12,611	3430	1105		1055	2681
12,612	3490	1121		1609	3434

one-half of the domain is analyzed. In Fig. 8, the left-hand side represents the crack lengths and the right-hand side gives the corresponding SIFs. The numbers within the ellipse denote the location and the magnitude of the maximum net ligament stress. The variations of SIF and the length of longest crack with number of cycles is presented in Fig. 9. The crack growth rate increases substantially at around 25,000 cycles. The first linkup occurs at 33,925 cycles, and then the cracks snap through all of the other ligaments almost instantaneously. This is both due to load redistribution as well as a substantial increase in crack tip SIF after the first linkup. The stress intensity factors increase with crack length and shoot up at linkup, thus increasing the crack growth rate to over 1/4 in./cycle. The load redistribution at first linkup shows that the next neighboring ligament has yielded. After the second linkup, the dominant crack tip SIF is high enough to snap through the third ligament within two cycles. Now, at the linkup of all cracks, there exists a central crack of 5 in. (12.7 cm). If there are no cracks in the next outer ligaments, the cracks can be treated as being arrested. However, if there is even a small crack, it can grow to the outermost hole in just a cycle, and then the outermost ligament yields, causing a complete failure of the panel. The significant observation is that the fatigue life of the coupon was only up to first linkup.

The load flow through the fasteners in the damaged row of fasteners at various stages is given in Table 1. Table 2 gives the rowwise load distribution at all of the stages. Interestingly, after first linkup, the damaged row takes up more load. The explanation may be as follows: As the cracks grow, the stiffness of the fasteners comes down, and they shed the load to the intact ligament, which now carries more stress. But at linkup the ligament can no longer

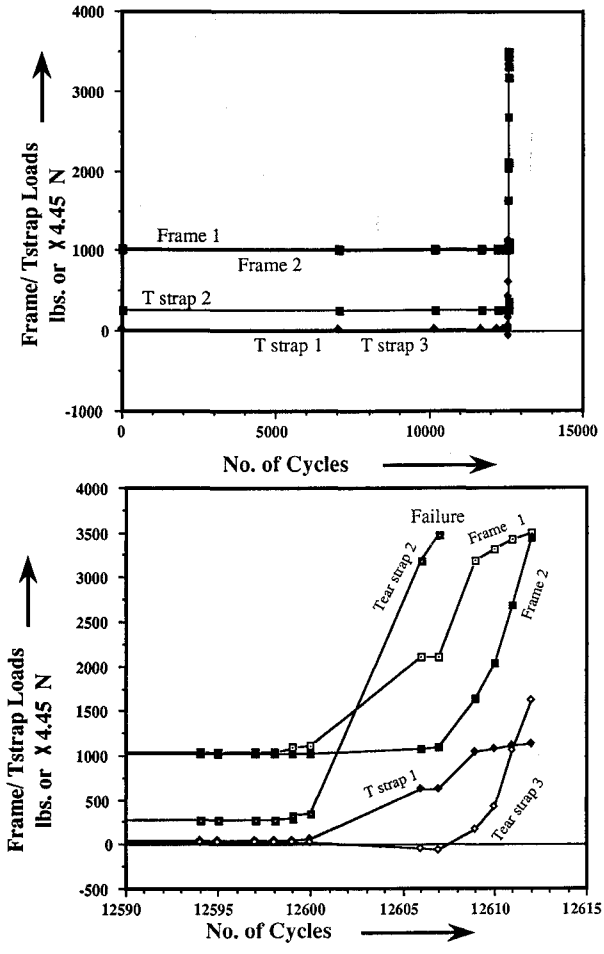

Fig. 13 Frame and the tear strap loads during fatigue.

take any load, and the entire load is diverted to the end rivets, which get heavily loaded.

The experimental effort[2] considered 10 specimens of this coupon. Out of these, five specimens were subjected to fatigue loading until failure, which occurred almost instantaneously after the first linkup. The five specimens demonstrated a fatigue life of 25,000, 105,700, 67,000, 41,400, and 57,370 cycles, respectively, leading to a mean life of 59,300 cycles. The analytical results give a life of about 34,000 cycles. Our analysis has given a conservative estimate that could be due to two main reasons. First, the plasticity effects on fatigue crack growth, such as the crack closure effects, have not been modeled in the analysis. Crack closure due to crack tip plasticity is known to reduce the effective stress intensity factor range over which fatigue crack growth occurs and thus to result in a prediction of slower growth. Previous investigations of static residual strength of damaged panels[1] did bring out the importance of plasticity in establishing the linkup criterion under stable growth due to static monotonic loading. Another factor could be that the crack tip in the experiment is initially blunt as it was generated due to spark erosion. Considering these points, the analysis seems to give a reasonably good estimate of fatigue life, with only a few hours of computational effort. By incorporating plasticity into the local analysis, we will be able to have better estimates.

Shell Panel Problem

The shell panel of Fig. 1 is now analyzed with the initial crack configuration of Fig. 2. The local and the global analyses are performed at crack length increments of 0.01 in. (0.0254 cm) and 0.04 in. (0.1016 cm) respectively. The fatigue damage is pictorially presented in Fig. 10. The corresponding crack lengths and the SIFs are plotted in Figs. 11 and 12, respectively, and their numerical values are listed in Table 3. Once again the same striking feature can be clearly seen; the "sudden death" of the panel. The first linkup occurs at 12,594 cycles, and then within 6 cycles, in each bay, all of the cracks link up to form a long crack. Within the next two cycles, the two long cracks across the frame coalesce to form a single dominant two-bay crack of over 20 in. (50.8 cm) in length. This dominant crack, due to its length and the associated tip SIF, has a growth rate of almost an inch/cycle. Even when the growth rate is less than an inch/cycle, it is large enough to reduce the length of the intact ligament, which fails under direct stress. Thus, with every cycle, the crack grows to the next fastener hole. At 12,607 cycles, when the crack spans over 15 holes in each bay, the midbay tear straps yield. From this stage onward, these are treated as having failed and modeled as not to take any more load (this is a conservative approach, as they might continue to bear some load). Because of this failure, the crack tip SIF suddenly shoots up and so does the crack growth rate. The tear straps do not appear to arrest the crack growth. By 12,611 cycles, there exists a full two-bay-long crack spanning from frame to frame. Thus, from the first linkup up to the formation of a two-bay crack, all it took was just 17 cycles. The analysis is stopped at this stage.

From Fig. 11, the crack closest to the frame has the lowest growth rate. The initially longer cracks (0.11 in.) are the fastest to grow and the first ones to link up (as intended at the time of initial crack configuration selection). Figure 12 shows the shootup of SIF after the first linkup. The presence of a frame does reduce the SIF (increasing the static residual strength) and does slow down the crack growth, but the effect adds virtually nothing to the countable cycles of residual life. These observations are, of course, within the limitations of applicability of the Paris equation to low cycle fatigue.

Figure 13 and Table 4 present the load flow pattern in the frames and the tear straps as the cracks grow. Yielding of the midbay strap can be seen to overload the intact frame/straps. Tear strap 3 shows a negative load for a small range; this could be due to the local in-plane bending moments being generated out of substantial load diversion.

Both the coupon and the shell panel with MSD are found to have fatigue lives only up to the first linkup. This is because after the first linkup the crack has a dominant length with high stress intensity factors. This is an important piece of information for the analyst involved in fatigue life estimation of similar structural components with widespread damage.

Conclusion

In a lap joint, the growth of multiple cracks emanating from a row of fastener holes has been investigated under cyclic loading. A flat plate coupon and a stiffened shell structure, typical of an airliner fuselage, were analyzed. The most important feature that emerges is that the fatigue life of the lap splice with widespread cracking is only up to the first linkup. Beyond this, the crack lengths, the corresponding stress intensity factors, and the crack growth rates become prohibitively high. A good linkup criterion is thus very important for residual life estimation of a structural component with multisite damage that is subject to fatigue loading. The second feature is that the frames or tear straps are hardly capable of arresting the growth of dominant cracks under fatigue loading.

Acknowledgments

The authors are grateful for the financial support from the Federal Aviation Administration (FAA) to the Center of Excellence for Computational Modeling of Aircraft Structures, Georgia Institute of Technology. They also acknowledge with pleasure the discussions and support from various colleagues, in particular Tom Swift and P. W. Tan of FAA and D. O. Potyondy and V. B. Shenoy of the Georgia Institute of Technology.

References

[1]Park, J. H., Singh, R., Pyo, C. R., Atluri, S. N., and Tan, P. W., "Residual Strength of Fuselage Panels with Wide-Spread Fatigue Damage," *Durability and Structural Reliability of Airframes*, edited by A. F. Blom, International Committee on Aeronautical Fatigue, 17th meeting (Stockholm, Sweden), Engineering Materials Advisory Services, UK, 1993, pp. 413–441.

[2]Molent, L., and Jones, R., "Crack Growth and Repair of MultiSite Damage of Fuselage Lap Joints," *Engineering Fracture Mechanics*, Vol. 44, No. 4, 1993, pp. 627–637.

[3]Ashwell, D. G., and Sabir, A. B., "A New Cylindrical Shell Finite Element Based on Simple Independent Shape Functions," *International Journal of Mechanical Sciences*, Vol. 14, No. 3, 1972, pp. 171–183.

[4]Swift, T., "Fracture Analysis of Stiffened Structures," American Society of Testing and Materials, STP 842, 1984, pp. 69–107.

[5]Park, J. H., and Atluri, S. N., "Fatigue Growth of Multiple Cracks near a Row of Fastener Holes in a Fuselage Lap Joint," *Proceedings of the International Workshop on Structural Integrity of Aging Airplanes*, edited by S. N. Atluri, P. Tong, and S. G. Sampath, Springer-Verlag, New York, 1992, pp. 91–116; also *Computational Mechanics*, Vol. 13, No. 3, 1993, pp. 189–203.

[6]Park, J. H., Ogiso, T., and Atluri, S. N., "Analysis of Cracks in Aging Aircraft Structures, With and Without Composite Patch Repairs," *Computational Mechanics*, Vol. 10, No. 3/4, 1992, pp. 169–202.

[7]Swift, T., "Damage Tolerance in Pressurized Fuselages," 11th Plantema Memorial Lecture, International Committee on Aeronautical Fatigue, 14th meeting (Ottawa, Canada), 1987.

[8]Swift, T., "Residual Strength of Stiffened Structures," Lecture at Georgia Inst. of Technology, Atlanta, GA, Feb. 10, 1993.

[9]Muskhelishvili, N. I., *Some Basic Problems of the Mathematical Theory of Elasticity*, Russian translation by J. R. M. Radok, Groningen, Noordhoff, 1953.

[10]Campbell, J. E., "Damage Tolerant Design Handbook," Metals and Ceramics Information Center, Battelle Columbus Labs., Columbus, OH, Jan. 1975, pp. 8.1–10.